

Estimation of heat source model parameters for twin-wire submerged arc welding

Abhay Sharma · Ajay Kumar Chaudhary ·
Navneet Arora · Bhanu K. Mishra

Received: 7 October 2008 / Accepted: 31 March 2009 / Published online: 24 April 2009
© Springer-Verlag London Limited 2009

Abstract Heat source models are mathematical expressions that represent the generation term in the fundamental heat transfer equation. Investigators have successfully demonstrated different heat source models for single-wire welding. The present investigation estimates the double ellipsoidal heat source model parameters for twin-wire application. The heat source model parameters have been estimated for varying set of welding conditions. It has been found that the heat source model parameters for twin-wire welding are different from the single-wire welding. Moreover, the heat source model parameters also depend upon process parameters. Effects of welding current, electrode polarity and wire diameter on the size of heat source model have been presented. Flux consumption is also found to play a significant role in deciding the heat source model parameters.

Keywords Twin-wire welding · Heat source model · Thermal cycle · Flux consumption

1 Introduction

Simulating the thermal input from the arc to the work-piece is one of the most important issues in the modelling of welding processes. The interaction of a heat source with a weld pool is a complex phenomenon and theoretical investigation by mathematical modelling provides an opportunity to understand the complex phenomenon that occurs during welding. The basic theory of heat flow developed by Fourier and applied to moving heat sources by Rosenthal [1] in the late 1930s to 1940s is one of the first analytical methods to calculate the thermal history of welds. The fundamental equation of heat transfer in a solid given by Fourier is as follows:

$$\frac{\partial H}{\partial t} = Q_g + \frac{\partial}{\partial x} \left(k \frac{\partial}{\partial x} \right) + \frac{\partial}{\partial y} \left(k \frac{\partial}{\partial y} \right) + \frac{\partial}{\partial z} \left(k \frac{\partial}{\partial z} \right) \quad (1)$$

where H and k represent enthalpy and thermal conductivity, respectively. The heat generation is represented by Q_g . During the investigation by Rosenthal [1], heat generation has been considered from a point source. The infinite temperature at heat source and temperature independent material thermal properties assumed in the Rosenthal's model increase the error as the heat source is approached. To overcome these limitations several researchers have used distributed heat source models. These heat sources, expressed in various mathematical forms, are used for heat generation term (Q_g) in Eq. 1. Investigators have used different heat sources like two dimensional disc model [2], Gaussian heat distribution [3], split heat source [4],

A. Sharma (✉)
Institute of Petroleum Technology Gandhinagar,
Raisan Village,
Gandhinagar 382 007 Gujarat, India
e-mail: abhay.sharma@iptg.ac.in

A. K. Chaudhary
Noida Institute of Engineering and Technology,
Greater Noida Phase-II,
201 305 Uttar Pradesh, India
e-mail: ajayagrohi@yahoo.co.in

N. Arora · B. K. Mishra
Department of Mechanical and Industrial Engineering,
Indian Institute of Technology Roorkee,
Roorkee 247 667, India

N. Arora
e-mail: arorafme@iitr.emet.in

B. K. Mishra
e-mail: bhanufme@iitr.emet.in

constant heat input [5], arc heat flux [6, 7], double ellipsoidal [8–11] etc. The resulting heat transfer equations have been solved using different numerical techniques like finite element method (FEM) and finite difference method. Goldak et al. [9] used FEM with double ellipsoidal heat source for 2-D analysis where as Robert et al. [12] used semi-discrete technique with hemispherical heat source for 3-D analysis. The Goldak’s double ellipsoidal heat source model [9], which is considered as a versatile model for various applications, is based on combination of two ellipsoids. These ellipsoids are geometrically different and having different heat density distribution as well. This model has been shown in Fig. 1. The front half is quadrant of one ellipsoidal source while the rear half is of another having semi-axis b_f and b_r , respectively. The power density function has been assumed as Gaussian distribution such that the power density falls to 5% of that at the centre of the heat source. The volumetric integration of power density gives the total power of the heat source Q_p . Thus, the heat density in the front at any point (x, y, z) at time t due to a heat source having power Q_p moving at speed v in y direction becomes as follows:

$$Q_g(x, y, z, t) = f_f \left(\frac{6\sqrt{3}Q_p}{\pi\sqrt{\pi ab_f c}} \right) e^{-\frac{3x^2}{a^2}} e^{-\frac{3(y-v)^2}{b_f^2}} e^{-\frac{3z^2}{c^2}} \quad (2)$$

The term f_f represents the fraction of heat supplied to the front of the arc. In Eq. 2, the parameters a, b and c that are expansion of heat source in lateral, longitudinal and depth directions respectively may have different values in front and rear quadrants. Indeed, in welding dissimilar metals, it may be necessary to use four octants, each with independent values of a, b and c . In case of similar metal, a and c are considered same and different b values are used in front and rear directions. Thus, b_r and f_r replaces b_f and f_f respectively for the rear half. Physically, these parameters are the radial dimensions of the molten weld pool in front, behind, to the sides and underneath the arc. The model parameters can be

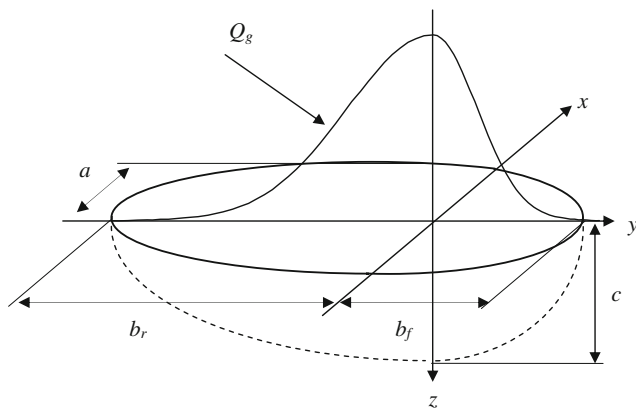


Fig. 1 Double ellipsoidal heat source

independently fixed so as the model can represent the heat source for different welding process. If the cross-section of the weld pool is known from the experiment, these data may be used to fix the heat source dimensions. In the previous investigation into single-wire submerged arc welding [9], quarter of weld width and twice of weld width have been prescribed for front and rear directions where as dimension in the transverse direction has been considered equal to half of weld width. Investigators have used the double ellipsoidal model for simulation of thermal history in welded joints produced by different welding processes. De et al. [13] used double ellipsoidal model for representation of heat source in LASER welding. Hongyuan et al. [14] modified the double ellipsoidal model for the situation where, under an external disturbance, the arc’s backbone is not perpendicular to the work surface. Slovacek et al. [15] used double ellipsoidal model for numerical simulation of manual metal arc welding and gas tungsten arc welding. In the recent past, Kermanpur et al. [16] investigated surface and volumetric heat sources for thermal simulation of gas tungsten arc welding. They showed that a fully volumetric arc heat input represents the best match to the welding of the thin-walled pipes.

Twin-wire application, as shown in Fig. 2, is slightly different from the single-wire. In case of twin-wire, two wires are fed through a common contact tube and power is supplied through single power source. During twin-wire welding, arcs pull together causing backward blow at the leading arc and forward blow at the trailing arc. That means the arcs are affected by each other. This phenomenon may affect the heat distribution pattern. In addition, twin-wire is meant for higher deposition and shallow penetration. Thus, the model parameters as indicated before may change. The moot point is whether the model parameters (a, b and c) suggested for single-wire application is applicable for twin-wire application. In the present investigation, this point has been studied by experimental measurement of thermal cycles and subsequent computation of the model parameters. In what follows, the experimental work regarding the present investigation has been described. It is followed by

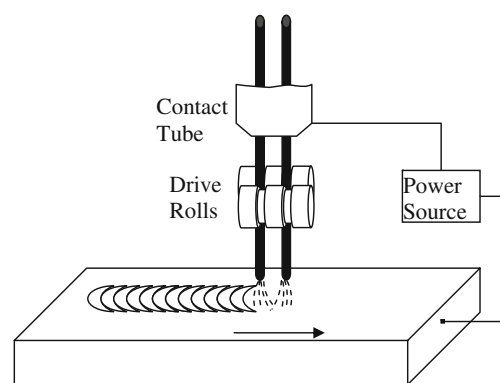


Fig. 2 Schematic diagram of twin-wire welding

description of heat source model for twin-wire welding. The results of computational exercise have then been presented and discussed. The paper has then been concluded with the generalised conclusions arrived at.

2 Experimental

The experimental work in the present investigation consists of measurement of transient temperature during the welding using twin-wire submerged arc welding. The specimens used for measurement of transient temperature were rectangular piece of mild steel of size $300 \times 200 \times 25$ mm. AWS/SFA A5.17 EH 14 grade filler wire was used along with basic flux. A submerged arc welding unit LE-18 (Messer-Griesheim) was used to deposit bead-on-plate welds. Axis-to-axis distance between wires has been kept as 9 mm. The flux had been baked for 2 h at 200°C before welding. Bead-on-plate welds were deposited using two wire diameters of 2 and 3.2 mm. Total 12 welds were deposited following the welding parameters given in Table 1. Thermocouple of type R (Pt–Pt and 13% Rh) with a diameter of 0.25 mm has been used for measuring the temperature variation during the welding. The thermocouples have been attached to the plates at three points situated within the body of the work-piece at centreline directly below the welding arc. The schematic diagram of the placement of thermocouples inside the plate has been shown in Fig. 3. These points were situated at different depths. A PC-based data acquisition system was used to sample the signal from the thermocouples. A picture of the experimental setup for temperature measurement is shown in Fig. 4. Some of the representative thermal cycles are shown in Figs. 5 and 6. Based on the experimental

Table 1 Experimental conditions

| S. No. | Current in (A) | Voltage (V) | Speed (cm/min) | Extension (mm) | Wire diameter (mm) | Polarity |
|--------|----------------|-------------|----------------|----------------|--------------------|----------|
| 1. | 400 | 32 | 40 | 40 | 2–2 | DCEP |
| 2. | 500 | 32 | 40 | 40 | 2–2 | DCEP |
| 3. | 600 | 32 | 40 | 40 | 2–2 | DCEP |
| 4. | 400 | 32 | 40 | 40 | 2–2 | DCEN |
| 5. | 500 | 32 | 40 | 40 | 2–2 | DCEN |
| 6. | 600 | 32 | 40 | 40 | 2–2 | DCEN |
| 7. | 600 | 32 | 40 | 40 | 3.2–3.2 | DCEP |
| 8. | 700 | 32 | 40 | 40 | 3.2–3.2 | DCEP |
| 9. | 800 | 32 | 40 | 40 | 3.2–3.2 | DCEP |
| 10. | 600 | 32 | 40 | 40 | 3.2–3.2 | DCEN |
| 11. | 700 | 32 | 40 | 40 | 3.2–3.2 | DCEN |
| 12. | 800 | 32 | 40 | 40 | 3.2–3.2 | DCEN |

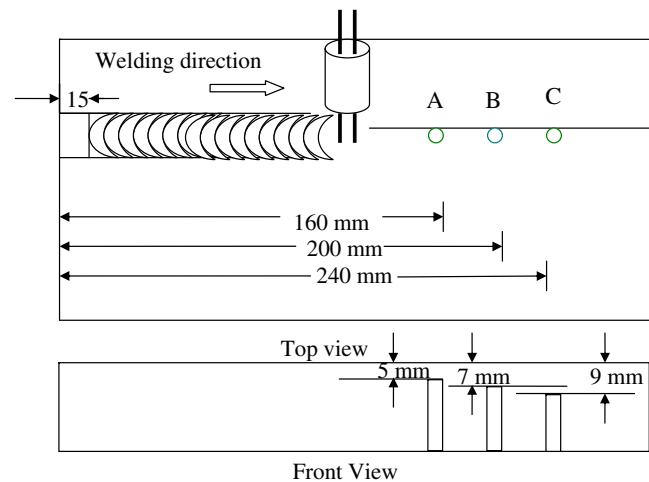


Fig. 3 Thermocouple placement

observations, heat source model parameters for twin-wire submerged arc welding have been estimated as given in the following section.

3 Heat source model

Due to close proximity of two wires during twin-wire application, they associate with a single weld pool and somehow act as a single elongated heat source [17]. Hence, a double ellipsoidal heat source, which has been found applicable in the case of single-wire application, may also be applied in this case. However, geometric parameters of the model would change. It is evident from the experimentally measured thermal cycles, as shown in Figs. 5 and 6, that the peak temperature is a momentary affair. The peak temperature mainly depends upon the amount of heat supplied to the work-piece at the very moment the arc acts over the point of consideration. It means that the peak temperature of any point is not affected by the pre- or the



Fig. 4 Experimental setup

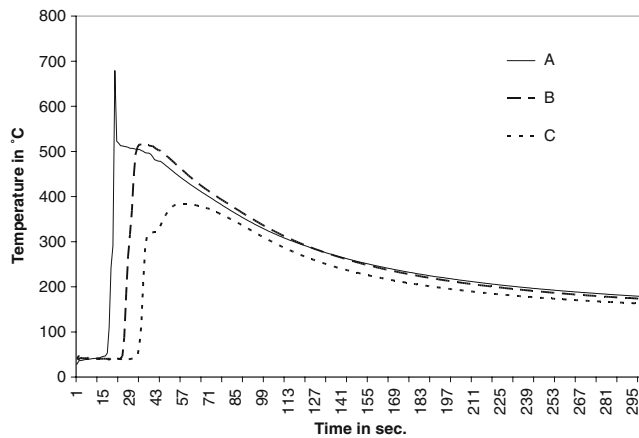


Fig. 5 Weld thermal cycle (3.2–3.2 mm wire DCEN, 600 A)

post-heating of the point when arc remains far from the point. Thus, the problem of model parameter identification can be simplified by steady-state heat transfer at the particular moment. An appropriate estimation of heat source parameters should result in appropriate prediction of peak temperatures at different points situated within the body of the work-piece. The heat conduction equation has been solved using control volume method in form of semi-discrete technique as given by Robert et al. [12]. In this technique, the body under consideration is discretized in small control volumes. The associated nodes are located at the geometric centre of the control volume for interior nodes. For control volumes that include geometric boundary of the work-piece, the associated nodes are considered on the surfaces. The thermal conductivity at the interface can be determined as the harmonic mean value as follows:

$$K(T_1, T_2) = \frac{2}{\frac{1}{K(T_1)} + \frac{1}{K(T_2)}} \tag{3}$$

where $K(T_1, T_2)$ is the thermal conductivity at the interface between nodes 1 and 2. As pointed by Patankar [18], this

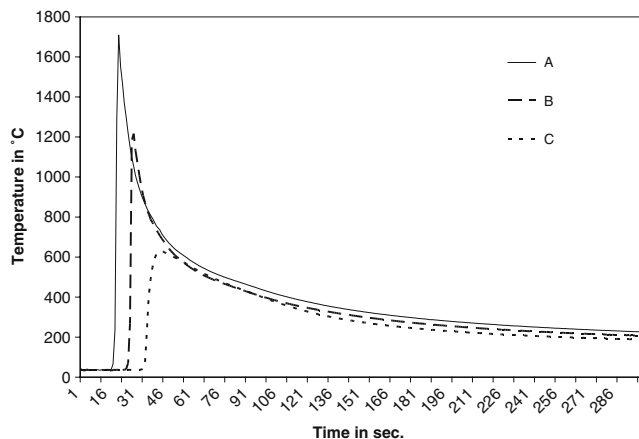


Fig. 6 Weld thermal cycle (3.2–3.2 mm wire, DCEN at 800 A)

ensures heat flux continuity at control volume interface, which is required for physical significance of discretization. The semi-discrete form of heat diffusion equation for 3-D heat transfer condition in steady state without any radiation yields the following:

$$\left\{ \frac{2K_{i,j,k}}{(\Delta x)^2} \right\} \left\{ \begin{aligned} & \frac{K_{i+1,j,k}(T_{i+1,k} - T_{i,j,k})}{K_{i+1,j,k} + K_{i,j,k}} + \frac{K_{i-1,j,k}(T_{i-1,k} - T_{i,j,k})}{K_{i-1,j,k} + K_{i,j,k}} \\ & + \frac{K_{i,j+1,k}(T_{i,j+1,k} - T_{i,j,k})}{K_{i,j+1,k} + K_{i,j,k}} + \frac{K_{i,j-1,k}(T_{i,j-1,k} - T_{i,j,k})}{K_{i,j-1,k} + K_{i,j,k}} \\ & + \frac{K_{i,j,k+1}(T_{i,j,k+1} - T_{i,j,k})}{K_{i,j,k+1} + K_{i,j,k}} + \frac{K_{i,j,k-1}(T_{i,j,k-1} - T_{i,j,k})}{K_{i,j,k-1} + K_{i,j,k}} \end{aligned} \right\} + Q_g = 0 \tag{4}$$

The task of solving heat conduction equation under varying model parameters has been completed through a code written in MATLAB software. For each welding condition, more than 10,000 combinations of parameters have been attempted which took more than 8 h of CPU time. The initial solution of the above equation resulted in certain amount of error in different cases. The error indicates the effect of flux during submerged arc welding. As soon as the arc acts at any point, the temperature reaches to the peak temperature. Simultaneously, flux also melts and in turn the entire heat supplied by the arc is not used for creation of peak temperature. However, the heat obtained by the flux is subsequently supplied to the work-piece in the later stages, but this heat is not available for peak temperature generation. Thus, peak temperature-based heat conduction analysis might result in some error in prediction. It has been found that if one more variable in the heat source model is added, the error goes considerably down. This variable named as ‘flux compensation factor (ϕ)’ is found to be different for different welding cases. This factor signifies the fraction of heat available to the work-piece for melting and generating peak temperature at the very moment the arc acts on the point of consideration. Pertaining to this factor, the modified heat source equation for front direction is as follows:

$$Q_g(x, y, z, t) = f_f \left(\frac{\phi 6\sqrt{3}Q_p}{\pi\sqrt{\pi ab_f c}} \right) e^{-\frac{3x^2}{a^2}} e^{-\frac{3(y-w)^2}{b_f^2}} e^{-\frac{3z^2}{c^2}} \tag{5}$$

The origin of the moving coordinate system has been located on the top surface of the work-piece at the midpoint in between the leading and the trailing wires. As shown earlier, 12 different welding conditions were applied to measure the temperature distribution at three different points. The heat conduction equation has been solved for all these cases by varying model parameters and the root-mean-square error in % (% RMSE) in the peak temperatures at three different

Table 2 Calculated model parameters

| Wire diameter (mm) | Polarity | Current (A) | Model parameters in mm | | | | ϕ | % RMSE |
|--------------------|----------|-------------|------------------------|-------|-------|------|--------|--------|
| | | | a | b_f | b_r | c | | |
| 2–2 | DCEN | 400 | 13.21 | 6.6 | 26 | 4.8 | 0.38 | 14.7 |
| | | 500 | 15.01 | 9.3 | 75 | 5.0 | 0.51 | 10.7 |
| | | 600 | 16.71 | 20.0 | 83 | 5.2 | 0.60 | 3.5 |
| | DCEP | 400 | 17.79 | 6.6 | 35 | 5.1 | 0.60 | 11.1 |
| | | 500 | 19.61 | 9.0 | 98 | 5.7 | 0.65 | 10.9 |
| | | 600 | 20.73 | 25.0 | 103 | 7.5 | 0.72 | 7.9 |
| 3.2–3.2 | DCEN | 600 | 19.37 | 4.8 | 38 | 8.0 | 0.49 | 16.5 |
| | | 700 | 19.83 | 4.9 | 89 | 8.9 | 0.71 | 8.0 |
| | | 800 | 20.18 | 5.0 | 90 | 9.4 | 0.77 | 6.2 |
| | DCEP | 600 | 18.31 | 4.5 | 36 | 9.6 | 0.61 | 5.8 |
| | | 700 | 19.10 | 4.7 | 38 | 10.1 | 0.89 | 9.4 |
| | | 800 | 19.18 | 4.7 | 76 | 10.9 | 0.93 | 1.5 |

a half of weld width, c depth of penetration

points has been computed. Based on these results, final model parameters have been found. The model expansion in transverse direction, i.e., a has been considered constant as half weld width. The value of b_f and b_r has been taken as 0.6 and 1.4, respectively as mentioned in the literature [12]. This consideration is based upon previous investigation into simulation of behaviour of leading and trailing arcs in twin-wire welding [19] that indicated that leading and trailing arcs share 30% and 70%, respectively of the total heat. Model parameters in the other directions, namely, b_p , b_f and c along with the flux compensation factor (ϕ) are varied at regular intervals and the resulting % RMSE has been computed. This has been repeated for all the 12 conditions. The best model parameters and related error for each case have been given in the Table 2. The overall performance of the considered approach for heat source model develop-

ment and subsequently prediction of peak temperature is well-evidenced from Fig. 7. It can be seen that predicted peak temperatures are in good agreement with the actual peak temperatures. It is evident from the Table 2 that the model is self-validating and in most of the cases % RMSE is less than 10%. In some of the cases, particularly lower currents, it is higher than 10%. Nevertheless, this is quite a satisfactory result as error up to 100°C is acceptable for welding thermal modelling [11]. Obviously, at lower current when the temperatures are lower, the amount of acceptable % error also increases. Thus, the estimated parameters can be considered as representative of heat source model for twin-wire welding. The subsequent section further discusses the outcomes of the present investigation.

4 Results and discussion

The significant outcome of the present investigation is the difference between the model parameters of single and twin-wire welding heat source model. During previous investigation with single-wire welding [9], under given welding condition (single weld), values of model parameters a , b_f and b_r , have been suggested equal to half of weld width, quarter of weld width and twice of weld width, respectively. Thus, the model parameters in this particular case follow the relation $b_f/a = 0.5$ and $b_r/a = 4$. However, these relations represent a particular welding condition. It is evident from Table 2 that under varying welding conditions the same ratios do not hold good. The ratios b_f/a and b_r/a are found varying between 0.24 to 1.20 and 1.96 to 4.99, respectively. Thus, difference between the model parameters of single and twin-wire welding along with dependence of model parameters on welding conditions is established.

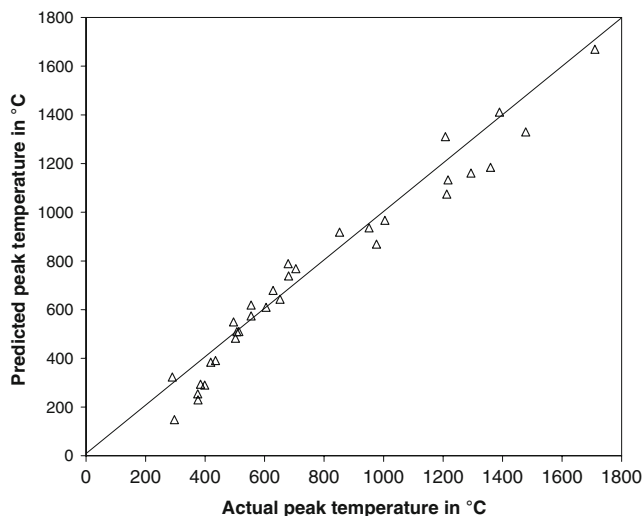


Fig. 7 Comparison of actual and predicted peak temperatures

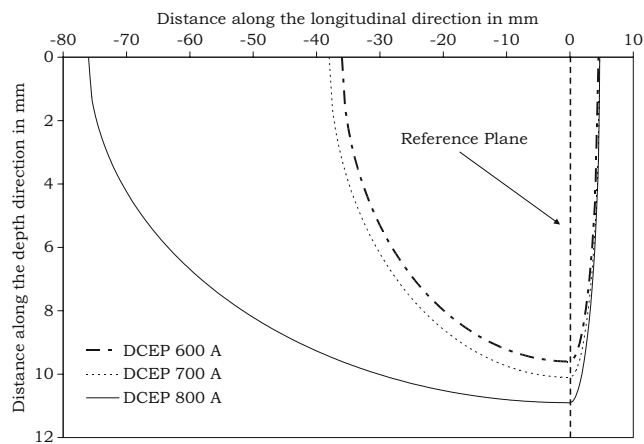


Fig. 8 Effect of current on heat source (3.2–3.2 mm wire combination DCEP)

The heat source model parameters under different welding conditions indicate expansion of heat in different directions. It is evident from Fig. 8 that the depth of heat source increases with the current. On the other hand, change in expansion of heat source in the front direction is not that much significant and it remains almost constant. However, the expansion in the rear direction is greatly affected by the current and a drastic increase is evidenced with increase in the current. These outcomes can be justified on the basis of physics of the process. It is well known that increment in the current increases the current density in the welding wire, which facilitates the increment in the penetration. In turn, the heat source attains larger depth with increase in the current. The expansion of heat source in the front direction can be attributed to two factors. In the front portion of the arc, metal remains in comparatively cold condition, which concentrates the arc. The second reason is due to the mechanism of twin-wire welding. Due to same polarity, the arcs are subject to arc

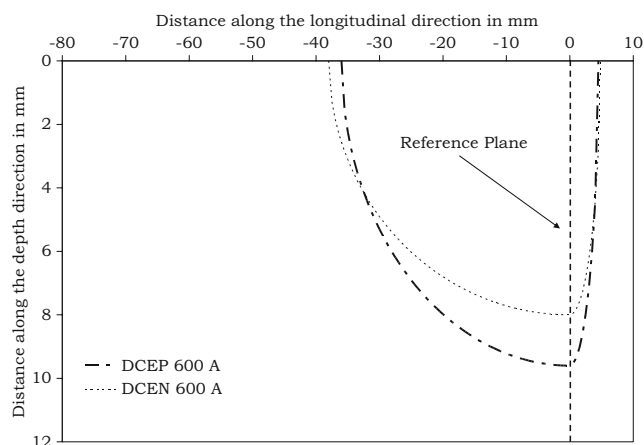


Fig. 9 Effect of polarity on heat source (3.2–3.2 mm wire combination)

blow in the inward direction. This further contracts the arc and results in lesser expansion. The model parameter in the rear direction is largely affected by current. The reason behind this outcome is the fact that higher current melts more metal, as well as the amount of heat supplied to the work-piece also increases. This results in more molten metal available beneath the arc and the size of weld puddle increases. This behaviour can be justified on the basis of fluid flow patterns during submerged arc welding, which has been studied by Mori and Horii [20]. According to them, a depression is formed at the forward edge of the weld pool and metal that is melted at the front of the pool flows rearward underneath and either side of the depression. This eventually results in higher expansion of the heat source in the rear direction.

Figure 9 shows the effect of polarity on heat source for 3.2–3.2 mm wire combination. It is evident that expansion in the depth direction is more in the case of direct current electrode positive (DCEP). This is due to the fact that DCEP produces more penetration, while in case of direct current electrode negative (DCEN) more filler material is melted and lesser penetration is achieved. As discussed earlier, the expansion of heat source in the front direction is not much affected by the welding conditions and the same is true for different polarities also. However, the expansion in the rear direction is affected by the polarity. The reason being that the DCEN melts more material that has the tendency to flow in the rear direction; in turn heat source is larger in the rear direction for the case of DCEN. However, a different observation is observed in case of the DCEN with smaller wire diameter (2–2 mm). It is evident from Table 2 that the size of heat source in all the three directions, i.e., front, rear and depth directions are smaller with DCEN. The DCEN and smaller wire diameter both yield more melting of filler wire. It seems that the excess molten metal hinders the heat flow to the base metal. Moreover, the flow of molten metal in the rear direction is also hampered. Thus, the dimension of heat source in the rear direction is found smaller with DCEN in case of 2–2 mm wire combination.

Figure 10 describes the effect of wire diameter on heat source. It is evident that smaller wire diameter produces less expansion of the heat source in the depth direction; where as in the front and rear directions, small wire diameter gives more expansion. The smaller wire diameter results in more melting of the filler material that flows in the either direction of the arc. Thus, the expansion in the front and rear direction with small wire diameter is found more. On the other hand, due to more melting of filler wire less energy is provided to the base metal, thus, less penetration is observed with smaller wire diameter. In turn, the expansion in the depth direction with small wire diameter (2–2 mm) is found lesser compared to larger wire diameter (3.2–3.2 mm).

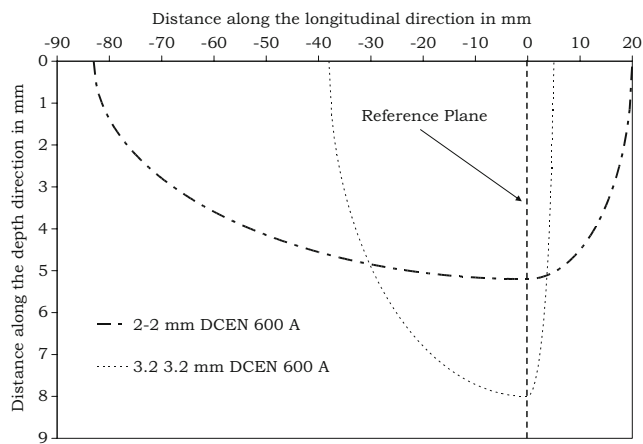


Fig. 10 Depth of heat source at different wire combinations

One of the important outcomes of this study is role of flux in producing peak temperatures. Figure 11 depicts the flux compensation factor (ϕ) for different welding conditions. This factor signifies the instantaneous amount of the heat available to the work-piece, while the flux has consumed the remaining part. It is evident that increment in current increases the factor at either polarities and at both wire combinations. This is due to increase in current which results in increase in the total amount of the heat. At the same time, the width of weld bead remains almost same and penetration increases. The net effect is in the form of more availability of heat to the work-piece and in turn ϕ increases. It is to be further noted that this factor has higher value at DCEP. This is due to the reason that DCEP melts less filler metal that keeps the surface area of the weld bead smaller and in turn less flux is consumed due to lesser area of contact. In addition, DCEP produces deeper penetration that provides more heat to the work-piece. As defined earlier, the flux compensation factor (ϕ) signifies

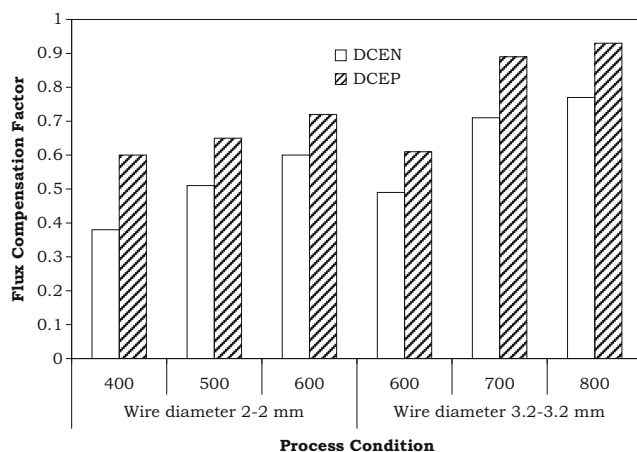


Fig. 11 Effect of welding conditions on flux compensation factor

the fraction of heat available to the work-piece for melting and generating peak temperature, thus, flux compensation factor (ϕ) achieves higher value with DCEP.

It can be found in literature that the flux consumption depends upon heat input, electrode polarity and wire diameter [21]. The same reasons are also responsible for alteration in heat transfer pattern. Thus, in order to assess the effect of flux consumption on the heat transfer pattern, effect of wire diameter and heat input must be secluded. It is evident that for the same wire diameter and current value (as shown in Fig. 11), ϕ is found higher for DCEP. It is also known that DCEP consumes less flux. Thus, more heat is supplied to the work-piece and ϕ has been found higher in case of DCEP. In case of smaller wire diameter the ϕ for the same current value (600 A) is found to be more than the other case. It seems that larger wire diameter increases the spread of the arc in lateral directions in turn more flux is consumed. Thus, lesser heat is available to the work-piece; eventually, ϕ achieves higher value at smaller wire diameter.

The discussion above lead to an important outcome that heat conduction equation solution for a given welding condition depends upon the surroundings. This becomes more important in case of submerged arc welding as flux is a good consumer of heat. Flux consumption is known to be a function of process parameters [21]. Thus, heat transfer model should be constructed keeping process conditions and the surrounding effects in consideration. Moreover, twin-wire welding results in more deposition of material that affects the flux consumption and heat distribution pattern as well. Thus, heat distribution pattern in a work-piece during the twin-wire welding becomes more dependent on the surroundings. The present investigation attempted to capture the same. The developed approach would also be useful in the future research in heat transfer modelling of other welding process.

5 Conclusions

1. The peak temperature-based approach for estimation of heat source model parameters is elaborative and tries to identify heat source model parameters according to the welding conditions.
2. Heat source model parameters for twin-wire welding are quite different from the single-wire heat source model. Due to mutual interaction between two wires, more melting and less penetration previous heat source model parameters for single-wire welding requires to be modified for twin-wire welding.
3. Effect of flux consumption on the heat transfer pattern can be quantified by appropriate compensation in the heat source model.

4. Static analysis considering stationary heat source is a simple and less time-consuming approach towards the identification of heat source parameters. This approach is quiet successful in understanding the mechanism of process variations like twin-wire submerged arc welding.

Acknowledgement This work has been carried out as a part of a research project funded by Department of Science and Technology, Government of India under the project number SR/S3/MERC-21/2005. The authors would like to thank All India Council for Technical Education (AICTE), Government of India, for supporting one of the authors (AS) during the period of this research.

References

- Rosenthal D (1946) The theory of moving sources of heat and its application to metal treatments. *Trans ASME* 68:849–866
- Pavelic V, Tanbakuchi R, Uyehara OA, Myers PS (1969) Experimental and computed temperature histories in gas tungsten-arc welding of thin plates. *Weld J* 48(7):295s–305s
- Eager TW, Tasi NS (1983) Temperature fields produced by travelling distributed heat source. *Weld J* 12:346s–354s
- Wahab MA, Painter MJ, Davies MH (1998) The prediction of the temperature distribution and weld pool geometry in the gas metal arc welding process. *J Mater Process Technol* 77(1):233–239. doi:10.1016/S0924-0136(97)00422-6
- Murugan S, Kumar PV, Raj B, Bose MSC (1998) Temperature distribution during multipass welding of plates. *Int J Press Vessels Pip* 75(12):891–905. doi:10.1016/S0308-0161(98)00094-5
- Choo RTC, Szekely J, Westhoff RC (1992) On the calculation of the free surface temperature of gas-tungsten-arc weld pools from first principles. *Metall Trans* 23B:357–384
- Fan HG, Tsai HL, Na SJ (2001) Heat transfer and fluid flow in a partially or fully penetrated weld pool in gas tungsten arc welding. *Int J Heat Mass Transfer* 44:417–428. doi:10.1016/S0017-9310(00)00094-6
- Duranton P, Devaux J, Robin V, Gilles P, Bergheau JM (2004) 3D modeling of multipass welding of 316L stainless steel pipe. *J Mater Process Technol* 153:457–463. doi:10.1016/j.jmatprotec.2004.04.128
- Goldak J, Chakravati A, Bibby M (1984) A new finite element model for welding heat sources. *Metall Trans* 15B:299–305
- Wen SW, Hilton P, Farrugia DCJ (2001) Finite element modelling of a submerged arc welding process. *J Mater Process Technol* 119(1):203–209. doi:10.1016/S0924-0136(01)00945-1
- Nguyen NT, Ohta A, Matsuoka K, Suzuki N, Maeda Y (1999) Analytical solutions for transient temperature of semi-infinite body subjected to 3-D moving heat sources. *Weld J* 78(8):265–274
- Ule RL, Joshi Y, Sedy EB (1990) A new technique for three dimensional transient heat transfer computations of autogenous arc welding. *Metall Trans* 21B:1033–1047
- De A, Maiti SK, Walsh C, Bhadeshia HDKH (2003) Finite element modelling of laser spot welding. *Sci Technol Weld Join* 8(5):377–384. doi:10.1179/136217103225005570
- Fang H, Meng Q, Xu W, Ji S (2005) New general double ellipsoid heat source model. *Sci Technol Weld Join* 10(3):361–368. doi:10.1179/174329305X40705
- Slováček M, Diviš V, Junek L, Ochodek V (2005) Numerical simulation of the welding process—distortion and residual stress prediction, heat source model determination. *Weld World* 49:15–29
- Kermanpur A, Shamanian M, Esfahani Yeganeh V (2008) Three-dimensional thermal simulation and experimental investigation of GTAW circumferentially butt-welded Incoloy 800 pipes. *J Mater Process Technol* 199:295–303. doi:10.1016/j.jmatprotec.2007.08.009
- Hinkel JE, Forsthoefel FW (1976) High current density SAW with twin electrodes. *Weld J* 3:175–180
- Patankar SV (1980) Numerical heat transfer and fluid flow. Hemisphere, New York, pp 25–61
- Sharma A., Arora N. and Gupta S. R., Simulation of behaviours of leading and trailing arcs during submerged twin arc welding, International Institute of Welding, Document No. ICRA-2005-IND-06
- Lancaster JF (1984) The physics of welding. Pergamon, UK, pp 242–243
- Sharma A, Arora N, Mishra BK (2008) Mathematical modeling of flux consumption during twin-wire welding. *Int J Adv Manuf Technol* 8(11–12):1114–1124. doi:10.1007/s00170-007-1181-y